Hindawi
Shock and Vibration
Volume 2023, Article ID 8080987, 12 pages
https://doi.org/10.1155/2023/8080987

Research Article

Spatial Variation Law of Blasting Vibration in Layered Strata under Blasting Excavation of Subway Tunnel

Zhen Zhang[1,2] **Chuanbo Zhou**[3] **Nan Jiang**[2,3] **and Yingkang Yao**[1]

[1]*State Key Laboratory of Precision Blasting, Jianghan University, Wuhan, Hubei 430056, China*
[2]*Engineering Research Center of Rock-Soil Drilling & Excavation and Protection, Ministry of Education, Wuhan, Hubei 430074, China*
[3]*Faculty of Engineering, China University of Geosciences, Wuhan, Hubei 430074, China*

Correspondence should be addressed to Zhen Zhang; zhangzhen9168@163.com

Received 18 September 2023; Revised 14 November 2023; Accepted 15 November 2023; Published 29 November 2023

Academic Editor: Marco Civera

Blasting vibration generated from blasting excavation of subway tunnel may endanger the adjacent structures buried in strata. To guarantee their safety and stability, it is crucial to understand the spatial variation law of blasting vibration in strata. In this paper, the blasting excavation of the large cross-sectional tunnel of Wuhan Metro Line 8 is studied. Three-dimensional finite element simulation is performed using the dynamic finite element program LS-DYNA, and its validity is verified by the field monitoring data. The spatial variation law of blasting vibration in layered strata is investigated through analyzed the distribution characteristic of blasting vibration in three directions, including the direction along the axis of the large cross-sectional tunnel, the direction perpendicular to the axis of the large cross-sectional tunnel, and the direction along the depth. A prediction model for blasting vibration velocity, which considers the impact of elevation differences, is established through dimensional analysis, enabling the prediction of blasting-induced vibrations at various depths in the layered strata.

1. Introduction

In China, metro lines located in urban areas are basically arranged in underground tunnels. Due to factors such as engineering geology and tunnel depth requirements, many tunnels need to pass through rocky areas. The drilling and blasting method, as an economical and efficient excavation technique, remains the main excavation method for tunnels in rock formations [1–3]. From the ground surface to the rock layer, where the tunnel is located, there may be multiple geological layers, and the geological layers above the tunnel are typically soil strata when near the ground surface.

During the blasting excavation of urban tunnels, the surrounding environment is complex, and there are a large number of pipelines and building structures around the blasting area. The load generated by the blasting excavation of the tunnel is transferred from the rock strata to the soil strata and finally reaches the ground surface. When structures (such as buried pipelines and foundations) are encountered along the propagation path of the blasting seismic wave, they will experience induced vibrations [4, 5]. If the blasting vibration intensity is significant, it can lead to structural damage, affecting the safety of the structures. Therefore, understanding the spatial variation law of blasting vibration in strata induced by tunnel blasting excavation is significant for the safety control of the structures adjacent to the blasting source.

In existing research, scholars usually fit the Sadovsky formula or other empirical vibration propagation formulas to get the blasting vibration propagation law on the ground surface based on the field monitoring data [2, 6–8]. Alternatively, researchers utilize numerical simulation methods to investigate the distribution pattern of blasting vibration on the ground surface [9–12]. A review of the currently available literature reveals that there is a lack of research on the propagation law of blasting vibrations in the geological layers [13, 14]. However, with an increase in urban blasting projects, it has become more common to encounter

structures such as pipelines and foundations near blasting sites, necessitating a deeper understanding of the spatial variation law of blasting vibrations in the rock and soil strata.

The main reason that there is limited research on the spatial variation law of blasting vibration in rock and soil layers is due to the difficulty in measuring blasting vibration in rock and soil strata using seismometers [14]. Monitoring blasting vibrations by burying blast vibration sensors in rock and soil strata presents a series of challenges, including difficulties in sensor placement, intricate preparation procedures, uncertainty in capturing vibration signals, and challenges in retrieving the vibration sensors. Moreover, due to restrictions in excavation equipment, the burial depth of vibration sensors is relatively shallow, and in urban areas, the hardened road surfaces and other issues may further hinder the burial of vibration sensors.

To investigate the spatial variation law of blasting-induced vibration in layered strata, a significant amount of blasting vibration data within the rock and soil strata is needed, which is difficult to obtain through on-site monitoring. In the present paper, the blasting excavation of the large cross-sectional tunnel of Wuhan Metro Line 8 is studied. The spatial variation law of blasting vibration in layered strata is investigated by numerical simulation with using ANSYS/LS-DYNA, and the validity of the numerical simulation is verified by using field monitoring data. In addition, a prediction model for blasting vibration velocity, which considers the impact of elevation differences, is established through dimensional analysis, enabling the prediction of blasting-induced vibrations at various depths in the layered strata.

2. Overview of the Large Cross-Sectional Tunnel Blasting Project

The large cross-sectional tunnel is a part of Wuhan Metro Line 8. As the tunnel is embedded in slightly weathered limestone, the drilling and blasting methods are selected during the construction process. Above the large cross-sectional tunnel, there is a civil air defense tunnel. Figure 1 depicts the spatial relation of the tunnel and the civil air defense tunnel. The large cross-sectional tunnel is 20.04 m in span and 12.78 m in height. The civil air defense tunnel is 2.3 m in span and 3.05 m in height. From top to bottom, it is 3.2 m thick of plain fill, 16.4 m thick of clay, and below 19.6 m is slightly weathered limestone.

According to the construction scheme, the working face of the large cross-sectional tunnel is segmented into three distinct sections, namely, the left, middle, and right sections, with each of these sections comprising three benches: the upper bench, middle bench, and lower bench. Cut blasting methodology is employed for the upper bench within each of the aforementioned sections, while a loose blasting technique is utilized for both the middle and lower benches. The upper bench of the left section of the tunnel is excavated first and cause larger vibration because of the clamping effect of the surrounding rock. The detailed dimensions of the large cross-sectional tunnel and the cut boreholes layout are shown in Figure 2. A total of eight cut boreholes, each measuring 250 centimeters in length, are utilized for the excavation process. A No. 2 emulsion explosive is selected for blasting, and each individual borehole is loaded with six rolls of explosives, resulting in a cumulative explosive charge of 14.4 kg. The detailed construction conditions can be found in Zhang et al. [15].

3. Validation of Modelling Techniques against Field Monitoring Data

The blasting vibrations in the civil air defense tunnel were monitored during the construction of the large cross-sectional tunnel. The monitoring points were positioned along the axis of the civil air defense tunnel, with the distance of 6 m between each monitoring point. The initial monitoring point was aligned with the working face of the upper bench on the left section, while the subsequent monitoring points were situated ahead of the working face where the excavation of the upper bench was not carried out. Figure 3 shows the blasting vibration gauges arrangement in the civil air defense tunnel. Table 1 provides the blasting vibration data obtained from on-site monitoring.

Based on field monitoring data, the authors validated the material models and parameters used in the numerical simulation [15]. A concise overview of the validation process is presented within this section. The authors developed a 3D finite element model for the blasting excavation of the large cross-sectional tunnel. The blasting vibration velocities in the civil air defense tunnel obtained from numerical simulation and field monitoring were compared. Figure 4(a) shows the comparison of the blasting vibration along the axis of the civil air defense tunnel. Figure 4(b) presents the relationships between the blasting vibration velocity and the scaled distance in the civil air defense tunnel obtained from field monitoring and numerical simulation. The comparison validated the modelling techniques and the verified material models and parameters can be applied to investigate the spatial variation law of blasting vibration in the layered strata. A comprehensive exposition of the modelling methodologies employed and the process of validation can be located within the work of Zhang et al. [15].

4. Spatial Variation Law of Blasting Vibration in Layered Strata

4.1. Numerical Model. The blasting excavation model of large cross-sectional tunnel is established to study the spatial variation law of blasting vibration in the strata. According to the survey report, the geological model of the site is generalized. From top to bottom, it is 3.2 m thick of plain fill, 16.4 m thick of clay, and below 19.6 m is slightly weathered limestone. Although each layer has slight undulations in different degrees according to the survey data, the degree of undulation is relatively slow, and the variation of the thickness of each stratum in the study area is limited. In order to keep the computational cost of the whole model within a controllable range, and to more typically represent the spatial variation law of blasting vibration in layered strata, the geological layers in the model are approximated as horizontal [16] and the civil air defense tunnel is not considered in this study. Figure 5 presents the 3D finite element

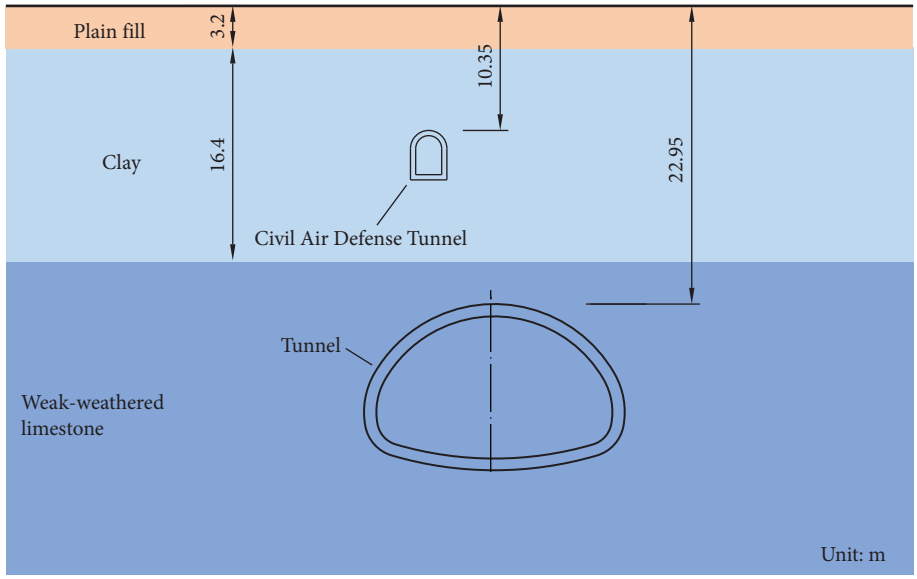

Figure 1: Spatial relation of tunnel and civil air defense tunnel.

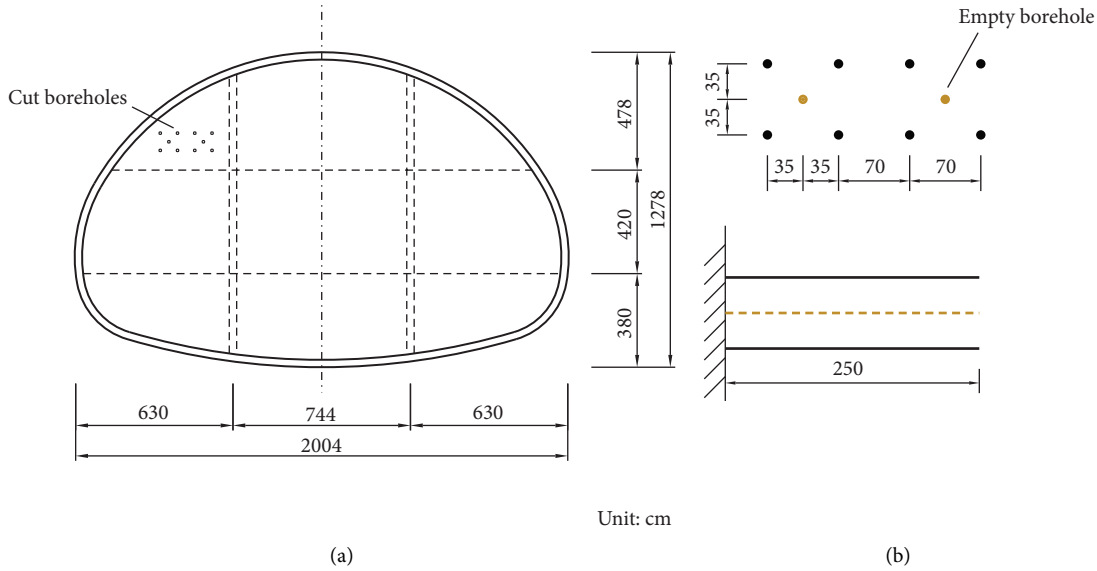

Figure 2: The large cross-sectional tunnel. (a) Different excavation sections of tunnel. (b) Cut boreholes.

model. The size of the model is 70 m × 45 m × 60 m. Point O in Figure 5 indicates the corresponding position on the ground surface directly above the blasting source. When the numerical simulation method is used to study blasting-related problems, the stress wave will be reflected when it reaches the boundary of the model due to the limited size of the established model, which will affect the calculation results. In order to eliminate the effect of stress wave reflection, a nonreflective boundary is applied around and at the bottom of the model [17, 18].

The materials used in the calculation model include explosives, slightly weathered limestone, plain fill, clay, and concrete. The models and parameters of each material can be found in Zhang et al. [15], and these models and parameters have been verified as described in Section 3.

4.2. Distribution Characteristic of Blasting Vibration in Strata along the Axis of the Large Cross-Sectional Tunnel. To study the distribution characteristic of blasting vibration in strata along the axis of the large cross-sectional tunnel, the vibration velocities at various depths in plain fill and clay layers are analyzed and compared with the vibration distribution on the ground surface along the axis of the tunnel. Figure 5 presents the arrangement direction of the ground surface vibration measuring points, and the arrangement of the measuring points in the soil is consistent with that on the ground surface. Figure 6 shows the depth of measurement line layout in the plain fill layer and clay layer.

Figure 7 presents the distribution patterns of vibrations on the ground surface and at different depths in the plain fill layer along the axis of the large cross-sectional tunnel. In

Figure 3: Blasting vibration monitoring.

Table 1: Blasting vibration of the civil air defense tunnel.

Excavation progress of upper bench of the left section (m)	Horizontal distance (m)	Blasting center distance (m)	Scaled distance ($m \cdot kg^{-1/3}$)	Vertical vibration velocity (cm/s)	Resultant velocity (cm/s)
92	6.15	14.91	6.13	4.03	4.67
	12.12	18.20	7.48	2.07	2.54
	18.11	22.64	9.30	1.35	1.82
98	6.32	14.98	6.16	4.85	4.94
	18.2	22.71	9.33	1.68	1.93
102	1.87	13.71	5.63	6.5	6.55
	6.45	15.03	6.18	5.28	5.33
	12.32	18.34	7.54	2.46	2.47
103.5	2.02	13.73	5.64	6.24	6.27
	6.51	15.06	6.19	5.7	5.84
	12.36	18.36	7.55	3.17	3.21
105.5	6.57	15.09	6.20	5.76	5.79
	18.34	22.82	9.38	1.56	1.68

Figure 7, the negative direction of the abscissa represents the back of the tunnel working face (excavated area), and the positive direction of the abscissa represents the front of the tunnel working face (unexcavated area).

It can be observed from Figure 7 that the vibration velocities on the ground surface are higher than that at the corresponding positions of 0.91 m, 1.83 m, and 2.74 m below the ground surface in the plain fill layer. The maximum surface vibration velocity can reach 3.36 cm/s. The main reason for the maximum surface vibration velocities is considered to be the superposition and reflection of stress waves at the free surface, with the strongest superposition effect occurring at the ground surface. In front of the tunnel working face, the ground vibration velocity continuously attenuates with the increasing distance from the tunnel working face. In the range of 0–10.33 m behind the tunnel working face, the ground vibration velocity decreases as the distance from the tunnel working face increases. When the distance between the monitoring point and the blasting source is greater than 10.33 m, the ground vibration velocity shows a trend of increasing first and then decreasing. Behind the tunnel working face is the excavated area. The upper surface of the cavity formed by the excavation provides a good free surface for the reflection of stress waves. The superposition of incident and reflected waves on the ground causes an increase in ground vibration velocity when the distance between the monitoring point and the blasting source is greater than 10.33 m. From this point of view, the excavated area exhibits an amplification effect (cavity effect) on ground vibrations.

The distribution patterns of vibrations at different depths in the plain fill layer along the axis of the large cross-sectional tunnel are similar with the vibration distribution pattern on the ground surface. The excavated area has an amplification effect on vibration at different depths in the plain fill layer. Notably, at a depth of 2.74 m from the ground surface, when

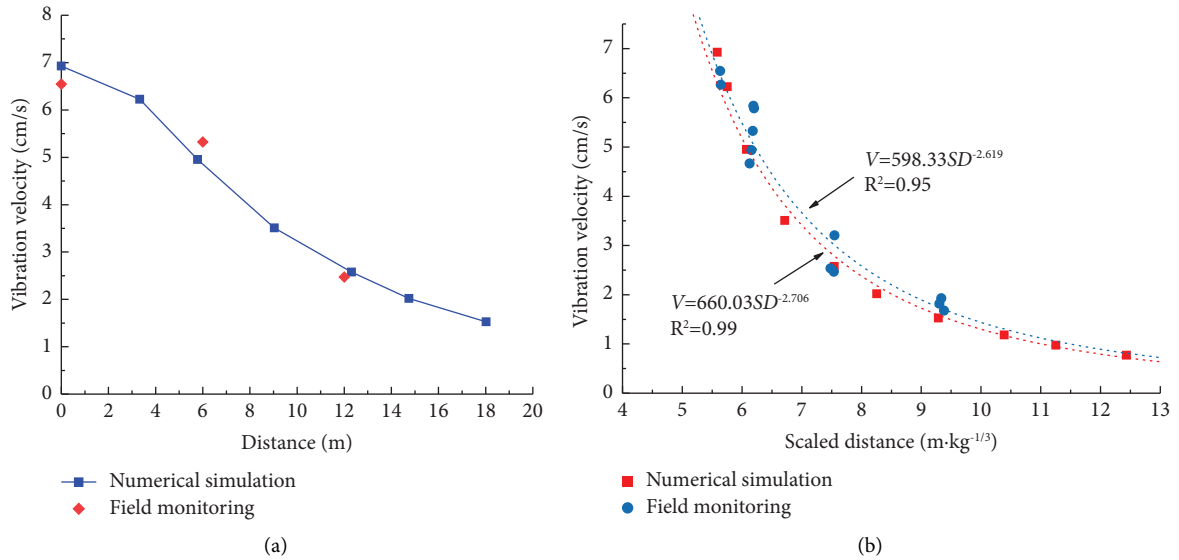

Figure 4: Comparison between numerical simulation and field monitoring [15]. (a) Vibration velocities along the axis of the civil air defense tunnel. (b) Vibration velocities versus scaled distances.

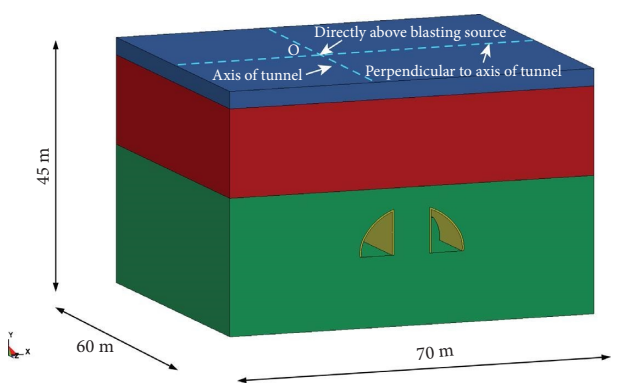

Figure 5: 3D finite element model.

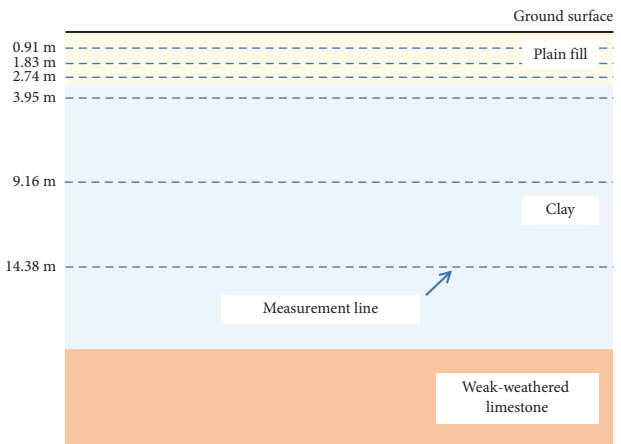

Figure 6: Layout of blasting vibration measurement lines.

the distance behind the working face is greater than 21 m and the distance in front of the working face is greater than 17.36 m, there is a minor increment in vibration velocity at monitoring points. At this depth, the blasting vibration measurement line is closer to the interface between the plain fill and clay layer, and the reflection and superposition of stress waves have a greater impact on the vibration velocity at positions farther from the tunnel working face. In the plain fill layer, stress waves continuously reflect and superimpose at the upper and lower interfaces, leading to the complexity of vibration propagation law within the plain fill layer. Along the axis of tunnel, there is no explicit magnitude relationship for the vibration velocity at the corresponding monitoring points at different depths.

Figure 8 provides the distribution patterns of blasting vibrations at the depths of 3.95 m, 9.16 m, and 14.38 m in the clay layer along the axis of the large cross-sectional tunnel. With the increase of distance from the ground surface (closer distance to the blasting source), the vibration velocity at corresponding monitoring points along the axis of the tunnel in the clay layer increases. At 1.6 m in front of the tunnel working face, the three curves all reached the peak value, and then the vibration velocity of the monitoring point decreased continuously with the increase of the distance from the tunnel working face. At a certain distance behind the tunnel working face, the vibration velocity of the corresponding monitoring points at different depths in the clay layer decreases with the increase of the distance from the working face. Beyond a certain distance, the vibration velocity of the monitoring point exhibits an initial increase followed by a decrease as the distance from the working face increases. This indicates that the cavity amplification effect of the excavated area has the same impact on the blasting vibration in the clay layer.

As the depth of the monitoring point in the clay layer increases, behind the working face, the initial distances at which the vibration velocity of the monitoring point increases are −10.33 m, −9 m, and −7.5 m, respectively. It can be seen that there is a monotonically decreasing relationship between the initial position, where the vibration velocity of the

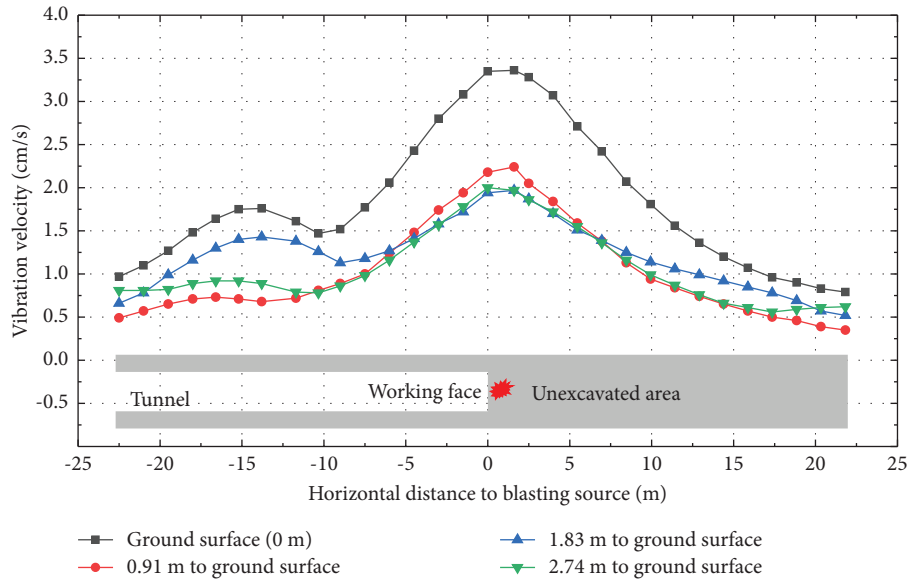

Figure 7: Blasting vibration in plain fill layer along the axis of tunnel.

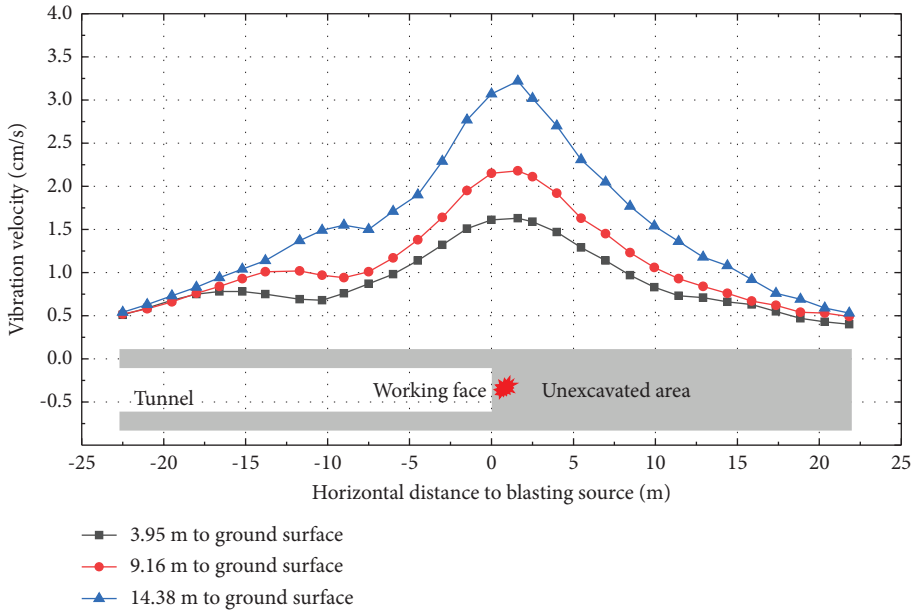

Figure 8: Blasting vibration in clay layer along the axis of tunnel.

monitoring point increases, and the depth of the measurement line in clay layer. Behind the working face, when the distance between the monitoring point and the face is large enough, the vibration velocities variation curves in the clay layer at different depths from the surface tend to converge.

4.3. Distribution Characteristic of Blasting Vibration in Strata Perpendicular to the Axis of the Large Cross-Sectional Tunnel. Figure 9 presents the distribution patterns of vibrations in the plain fill layer perpendicular to the axis of the large cross-sectional tunnel. In Figure 9, the negative direction of the abscissa indicates the left side of the blasting source, and the positive direction of the abscissa indicates the right side of the blasting source.

It can be seen that perpendicular to the axis of the large cross-sectional tunnel, the velocity at the position directly above the blasting source center is the largest on the measurement lines at different depths. In the direction perpendicular to the axis of the large cross-sectional tunnel, the vibration velocity of the monitoring point on the ground surface is greater than that of the corresponding position in the plain fill layer at different depths. The vibration velocities at corresponding positions on the left and right sides of measuring lines at different depths do not differ significantly, exhibiting a predominantly symmetrical distribution. With

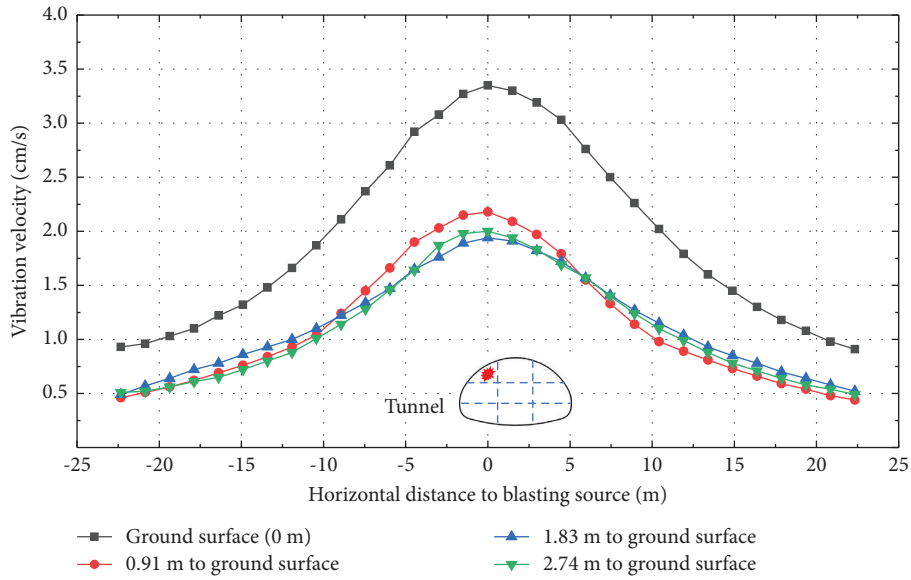

Figure 9: Blasting vibration in plain fill layer perpendicular to the axis of tunnel.

an increasing distance from the origin, vibration velocities at monitoring points on both sides demonstrate a trend of attenuation. In the plain fill layer, due to the reflection and superposition of the stress wave on the free surface and the plain fill-clay interface, the vibration velocity of the corresponding monitoring point at different measurement lines does not exhibit a monotonic relationship with increasing depth from the ground surface.

Figure 10 shows the vibration distribution in the direction perpendicular to the axis of the large cross-sectional tunnel in the clay layer at depths of 3.95 m, 9.16 m, and 14.38 m from the ground surface, respectively. The vibration velocity distribution pattern of different measurement lines in the clay layer is similar to that in the plain fill layer. However, the difference lies in the fact that, with an increase in distance from the ground surface, the particle vibration velocities at the corresponding positions at different depths exhibit a distinct increasing trend. At different depths, on both sides of the blasting source center, the amplitude of velocity increasement gradually decreases with the increase of the distance from the blasting source center.

4.4. Distribution Characteristic of Blasting Vibration in Strata along the Depth Direction. From Section 4.3, we know that the distribution characteristic of blasting vibration in the direction perpendicular to the axis of the tunnel shows a symmetrical pattern. Therefore, when studying the variation law of blasting vibration in the strata along the depth direction, only the measurement lines at the left side of the working face are investigated. The measurement lines are in the cross-section containing the working face, and their horizontal distances to the blasting source are 0 m, 4.47 m, 8.93 m, 13.41 m, and 17.88 m, respectively. Figure 11 shows the distribution of vibration velocity along the depth direction at different positions, with the dashed line indicating the interface between the plain fill layer and the clay layer.

It can be seen from Figure 11 that the vibration distribution along the depth direction presents a similar pattern at different horizontal distances from the blasting source. Herein, the vibration distribution law along the depth direction right above the blasting source is taken as an example for analysis. From the plain fill layer-clay layer interface to the ground surface, the distance between the monitoring points and the blasting source steadily increases. According to the conventional law, with the increase of the distance from the blasting source, the blasting vibration velocity should gradually decrease. However, in the plain fill layer, as the distance from the blasting source increases, the particle vibration velocity fluctuates in an oscillating manner. When reaching the ground surface, the particle vibration velocity reaches its peak. The reflection of the stress wave on the ground surface and the transmission and reflection at the interface between the plain fill layer and the clay layer induce a fluctuating pattern of velocity distribution in the plain fill layer.

Within the range of 4.69 m–3.20 m from the ground surface in the clay layer, the particle vibration velocity still shows an increasing trend with the increase of the distance from the blasting source. When the distance from the ground surface is greater than 4.69 m, the vibration velocity attenuation law is consistent with the conventional attenuation law. With the increase of the distance from the blasting source, the particle vibration velocity continuously decreases. The vibration velocity is at its minimum at 4.69 m from the ground surface. Hence, it is evident that the variation law of the particle vibration velocity is affected by the ground surface and the plain fill layer-clay layer interface, and the influence depth is about 4.69 m.

By comparing the vibration distribution along the depth direction at different horizontal distances from the blasting source, it can be found that as the horizontal distances from the blasting source increases, the vibration velocity of the corresponding point presents a decreasing trend. In the plain

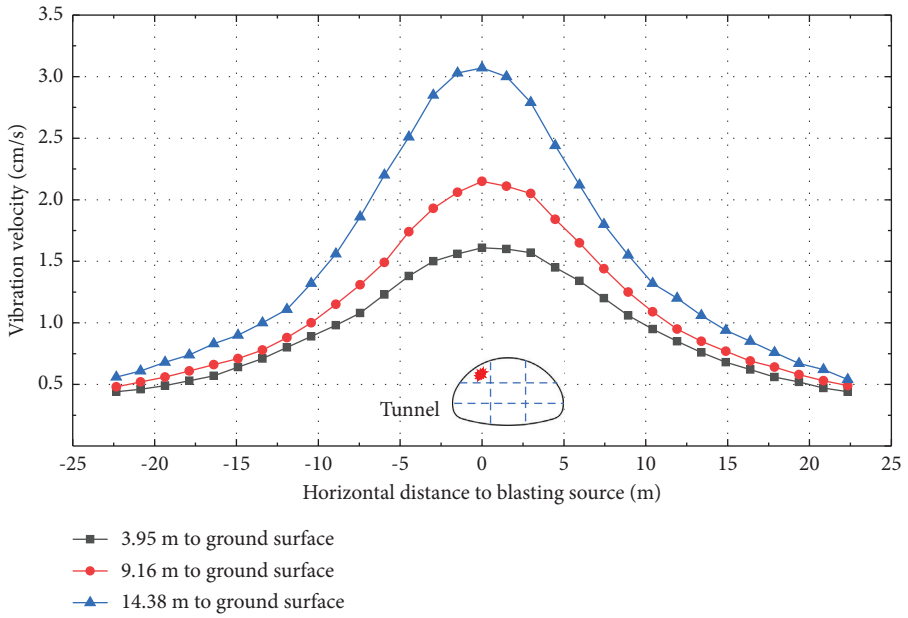

Figure 10: Blasting vibration in clay layer perpendicular to the axis of tunnel.

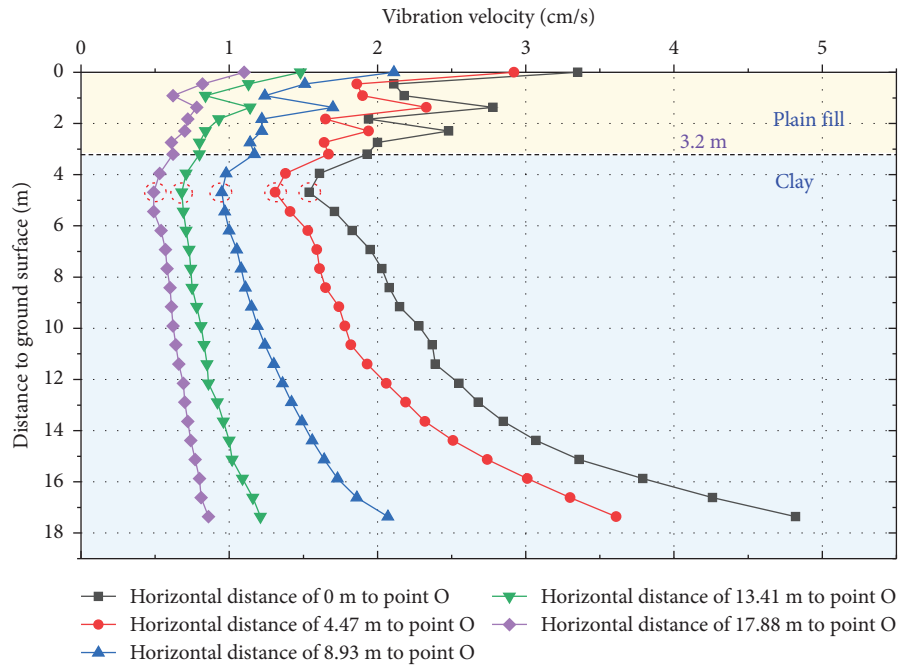

Figure 11: Blasting vibration along the depth direction.

fill layer, with the increase of the horizontal distances from the blasting source, the fluctuation of particle vibration velocity decreases continuously. Analyzing the influence depth of the ground surface and plain fill layer-clay layer interface on the variation of particle vibration velocity, it can be found that the influence depth is basically consistent at various distances from the blasting source, with an approximate value of 4.69 m. Table 2 provides the vibration velocity on ground surface and the vibration velocity at a distance of 4.69 m below the ground surface (minimum velocity) at various measurement lines. At different horizontal distances from the blasting source, the ratio of the vibration velocity at the ground surface to the vibration velocity at 4.69 m from the ground surface is in the range of 2.18 to 2.24. It can be seen that within the influence depth of the ground surface and the plain fill layer-clay layer interface, the ratio between maximum and minimum vibration velocities remains relatively stable.

Table 2: Vibration velocity at ground surface and 4.69 m away from ground surface.

Horizontal distance to the blasting source (m)	Vibration velocity at ground surface (cm/s)	Vibration velocity at 4.69 m away from ground surface (cm/s)	Vibration velocity ratio
0	3.35	1.54	2.18
4.47	2.92	1.31	2.23
8.93	2.11	0.95	2.22
13.41	1.48	0.68	2.18
17.88	1.1	0.49	2.24

5. Prediction Model of Blasting Vibration Velocity in Layered Strata

The peak particle vibration velocity is a main parameter to characterize the blasting vibration effect both domestically and internationally [19, 20], and it is affected by factors such as the blasting source and the transmission medium during the propagation process of blasting vibration. When studying the variation law of blasting vibration velocity, it is necessary to comprehensively consider the influence of these factors, but it is difficult to realize in practical engineering. Through a large number of experiments, the former Soviet scientist Sadovsky obtained an empirical formula that characterizes the propagation law of blasting vibration velocity, which has been widely used in engineering practice [21, 22]. However, the Sadovsky formula does not account for the influence of the elevation difference between the monitoring point and the blasting source, so there are limitations in predicting the blasting vibration at different depths in the strata. In this section, a blasting vibration velocity prediction model considering the influence of elevation difference is derived through dimensional analysis, which can be used as a reference for predicting the vibration velocity in strata during the blasting excavations of urban subway tunnels.

According to the existing research results concerning the attenuation law of blasting vibration, it can be known that the propagation and attenuation of blasting seismic waves in the stratum are affected by factors such as the blasting source, the characteristics of the stratum, and the distance from the blasting source [23–25]. The key variables affecting the propagation of blasting seismic waves are presented in Table 3.

Taking the peak particle vibration velocity (v) resulting from tunnel blasting as dependent variable, its function expression can be expresses as following according to Buckingham's Pi theorem of dimensional analysis [26]:

$$v = f(Q, c, \rho, r, H, t). \tag{1}$$

Taking Q, c, and r as independent dimensional quantities, and using π to represent dimensionless variables, we have

$$\begin{cases} \pi = \dfrac{v}{Q^{\alpha} r^{\beta} c^{\gamma}}, \\ \pi_1 = \dfrac{\rho}{Q^{\alpha} r^{\beta} c^{\gamma}}, \\ \pi_2 = \dfrac{H}{Q^{\alpha} r^{\beta} c^{\gamma}}, \\ \pi_3 = \dfrac{t}{Q^{\alpha} r^{\beta} c^{\gamma}}, \end{cases} \tag{2}$$

where α, β, and γ are undetermined coefficients. According to the principle of dimensional homogeneity:

$$\pi = \frac{v}{c}, \pi_1 = \frac{\rho}{\mathrm{Qr}^{-3}}, \pi_2 = \frac{H}{r}, \pi_3 = \frac{t}{\mathrm{rc}^{-1}}, \tag{3}$$

Substituting equation (3) into equation (1) yields:

$$\frac{v}{c} = f\left(\frac{\rho}{\mathrm{Qr}^{-3}}, \frac{H}{r}, \frac{t}{\mathrm{rc}^{-1}}\right). \tag{4}$$

Because the product and exponentiation of different dimensionless variables remain dimensionless, combining π_1 and π_2 results in the following new dimensionless variable:

$$\pi_7 = \left(\pi_2^{1/3}\right)^{\beta_1} \pi_3^{\beta_2} = \left(\frac{\sqrt[3]{\rho} r}{\sqrt[3]{Q}}\right)^{\beta_1} \left(\frac{H}{r}\right)^{\beta_2}. \tag{5}$$

When blasting seismic waves propagate in the same geological layer, ρ and c can be approximated as constants. Thus, from the above equation, it can be deduced that v has the following relationship with Q, r, and H:

$$v \sim \left(\frac{r}{\sqrt[3]{Q}}\right)^{\beta_1} \left(\frac{H}{r}\right)^{\beta_2}. \tag{6}$$

The relationship can be written in the following form:

$$\ln v = \alpha_1 + \beta_1 \ln\left(\frac{\sqrt[3]{Q}}{r}\right) + \left[\alpha_2 + \beta_2 \ln\left(\frac{H}{r}\right)\right]. \tag{7}$$

Table 3: Key independent variables associated with blasting vibration velocity.

Category	Independent variable	Dimension
Explosive parameters	Explosive mass Q	M
	Detonation time t	T
Location parameters	Horizontal distance between measuring point and blasting source r	L
	Elevation difference between measuring point and blasting source H	L
Medium parameters	Density of rock and soil ρ	ML^{-3}
	Velocity of blasting seismic wave c	LT^{-1}

Let $\ln v_0 = \alpha_1 + \beta_1 \ln(\sqrt[3]{Q}/r)$, then

$$\ln v_0 = \alpha_1 + \frac{\beta_1 \ln Q}{3} - \beta_1 \ln r. \tag{8}$$

In the above equation, $-\beta_1 \ln r$ represents the attenuation of blasting vibration velocity with respect to r, where β_1 reflects the attenuation index associated with site medium condition, and $\alpha_1 + (\beta_1 \ln Q)/3$ accounts for the combined impact of medium condition and explosive charge on the blasting vibration velocity.

Let $\ln k_1 = \alpha_1$, then

$$v_0 = k_1 \left(\frac{\sqrt[3]{Q}}{r}\right)^{\beta_1}. \tag{9}$$

Equation (9) is the classical Sadovsky formula that does not account for the elevation difference effect. Further transformation of equation (7) yields

$$\ln v = \ln v_0 + \left[\alpha_2 + \beta_2 \ln\left(\frac{H}{r}\right)\right]. \tag{10}$$

Let $\ln k_2 = \alpha_2$, then equation (10) can be transformed into

$$v = k_1 k_2 \left(\frac{\sqrt[3]{Q}}{r}\right)^{\beta_1} \left(\frac{H}{r}\right)^{\beta_2}. \tag{11}$$

Let $k = k_1 k_2$, then equation (11) can become

$$v = k \left(\frac{\sqrt[3]{Q}}{r}\right)^{\beta_1} \left(\frac{H}{r}\right)^{\beta_2}, \tag{12}$$

where k denotes the site influence coefficient, β_1 represents the attenuation coefficient, and β_2 reflects the impact coefficient associated with the elevation difference between the monitoring point and the blasting source.

When blasting seismic waves propagate outward from the blasting source, they pass through multiple geological layers. The attenuation of seismic waves varies in different strata. In the strata near the ground surface, the attenuation of blasting vibrations does not follow conventional law due to the reflection and superposition of stress waves. Therefore, it is necessary to predict blasting vibration velocities separately for different strata. The numerical simulation results are used here to fit the blasting vibration prediction model to predict the blasting vibration velocity in the strata.

According to the numerical simulation results, the blasting vibration velocity in the clay layer decreases continuously with the increase of the distance between the monitoring point and the blasting source, but in the plain fill layer, due to the reflection and superposition of the stress wave between the ground surface and the plain fill-clay interface, the blasting vibration velocity exhibits a fluctuating pattern. When fitting the blasting vibration attenuation model in plain fill layer, equation (12) cannot reflect the velocity fluctuation well, so only the vibration velocity at the peak of the fluctuation is considered for fitting, and the prediction model obtained is relatively safer. Table 4 presents the blasting vibration attenuation models in the plain fill layer and clay layer.

According to the obtained predictive model, when using the controlled variable method for analysis, it can be observed that in the clay layer, as the horizontal distance increases, the peak particle velocity decreases; with an increase in explosive charge, the peak particle velocity increases; and with an increase in elevation difference, the peak particle velocity decreases. These findings are consistent with the results of the earlier numerical analysis. In the plain fill layer, as the horizontal distance increases, the peak particle velocity decreases; with an increase in explosive charge, the peak particle velocity increases; and with an increase in elevation difference, the peak particle velocity actually increases. These observations align with the overall trend observed in the numerical simulation results. The correlation coefficients in plain fill and clay layers are 0.9724 and 0.9435, respectively, indicating that equation (12) fits the blasting vibration velocity well with a good level of correlation.

It is worth noting that in this project, the thickness of plain fill layer is only 3.2 m. There is an overall trend of increasing blasting vibration velocity with an increase in distance from the blasting source in the depth direction. However, as the thickness of the top soil layer increases, the influence depth of the stress wave reflection and superposition is limited. In these cases, the overall range of increase in blasting vibration velocity will be smaller than the thickness of the top soil layer as the distance from the blast source increases and the prediction of vibration velocity for the top soil layer should be carried out based on the actual circumstances.

Table 4: Blasting vibration velocity attenuation predictive model.

Geological layer	Blasting vibration attenuation model	Correlation coefficient
Plain fill	$v = 3.3\mathrm{E}^{-5}\,(\sqrt[3]{Q}/r)^{-4.283}\,(H/r)^{4.947}$	0.9724
Clay	$v = 38.92\,(\sqrt[3]{Q}/r)^{2.201}\,(H/r)^{-1.293}$	0.9435

6. Conclusions

Based on the blasting excavation of the large cross-sectional tunnel, the spatial variation law of blasting-induced vibration in layered strata is investigated. Blasting vibration prediction model consider the impact of elevation differences is established through dimensional analysis. The main conclusions of this paper are as follows:

(1) Along the axis of the large cross-sectional tunnel, the vibration velocities on the ground surface are higher than that at corresponding positions in plain fill layer. The excavated area exhibits an amplification effect on vibration at different depths both in plain fill and clay layer.

(2) Along the direction perpendicular to the axis of the large cross-sectional tunnel, the velocity at the position directly above the blasting source center is the largest on the measurement lines at different depths. The vibration velocities exhibit a predominantly symmetrical distribution in plain fill layer and clay layer.

(3) Along the depth direction, the ground surface and the plain fill layer-clay layer interface induce a fluctuating pattern of velocity distribution in the plain fill layer and their influence depth is about 4.69 m.

(4) By theoretical analysis, with elevation difference taken into account, a blasting vibration velocity prediction model is established. The blasting vibration attenuation models in the plain fill layer and clay layer are proposed and can be used to conveniently assess and control the potential risk of blasting seismic effect.

Data Availability

The data used to support the findings of this study are included within the article.

Conflicts of Interest

The authors declare that they have no conflicts of interest.

Acknowledgments

The study was sponsored by the National Natural Science Foundation of China (42102329), Hubei Provincial Natural Science Foundation (2023AFB1075), Knowledge Innovation Program of Wuhan (2023020201020445), and Open Fund of Engineering Research Center of Rock-Soil Drilling & Excavation and Protection, Ministry of Education (202213).

References

[1] O. Yilmaz and T. Unlu, "An application of the modified Holmberg–Persson approach for tunnel blasting design," *Tunnelling and Underground Space Technology*, vol. 43, pp. 113–122, 2014.

[2] X. Tian, Z. Song, and J. Wang, "Study on the propagation law of tunnel blasting vibration in stratum and blasting vibration reduction technology," *Soil Dynamics and Earthquake Engineering*, vol. 126, Article ID 105813, 2019.

[3] J. Yu, Z. Zhou, X. Zhang, X. Yang, J. Wang, and L. Zhou, "Vibration response characteristics of adjacent tunnels under different blasting schemes," *Shock and Vibration*, vol. 2021, Article ID 5121296, 13 pages, 2021.

[4] R. He, N. Jiang, D.-W. Li, and J.-F. Qi, "Dynamic response characteristic of building structure under blasting vibration of underneath tunnel," *Shock and Vibration*, vol. 2022, Article ID 9980665, 13 pages, 2022.

[5] N. Jiang, B. Zhu, C. Zhou et al., "Safety criterion of gas pipeline buried in corrosive saturated soft soil subjected to blasting vibration in a coastal metro line," *Thin-Walled Structures*, vol. 180, Article ID 109860, 2022.

[6] U. Ozer, A. Kahriman, M. Aksoy, D. Adiguzel, and A. Karadogan, "The analysis of ground vibrations induced by bench blasting at Akyol quarry and practical blasting charts," *Environmental Geology*, vol. 54, no. 4, pp. 737–743, 2008.

[7] R. Kumar, D. Choudhury, and K. Bhargava, "Determination of blast-induced ground vibration equations for rocks using mechanical and geological properties," *Journal of Rock Mechanics and Geotechnical Engineering*, vol. 8, no. 3, pp. 341–349, 2016.

[8] H. Agrawal and A. K. Mishra, "Modified scaled distance regression analysis approach for prediction of blast-induced ground vibration in multi-hole blasting," *Journal of Rock Mechanics and Geotechnical Engineering*, vol. 11, no. 1, pp. 202–207, 2019.

[9] Y. L. Gui, Z. Y. Zhao, L. B. Jayasinghe, H. Y. Zhou, A. T. C. Goh, and M. Tao, "Blast wave induced spatial variation of ground vibration considering field geological conditions," *International Journal of Rock Mechanics and Mining Sciences*, vol. 101, pp. 63–68, 2018.

[10] A. Haghnejad, K. Ahangari, P. Moarefvand, and K. Goshtasbi, "Numerical investigation of the impact of rock mass properties on propagation of ground vibration," *Natural Hazards*, vol. 96, no. 2, pp. 587–606, 2019.

[11] S. Chai, W. Tian, L. Yu, and H. Wang, "Numerical study of ground vibrations caused by cylindrical wave propagation in a rock mass with a structural plane," *Shock and Vibration*, vol. 2020, Article ID 4681932, 9 pages, 2020.

[12] D. Guo, W. Xiao, D. Guo, and Y. Lu, "Numerical simulation of surface vibration propagation in tunnel blasting," *Mathematical Problems in Engineering*, vol. 2022, Article ID 3748802, 10 pages, 2022.

[13] C. Wu, Y. Lu, H. Hao, W. K. Lim, Y. Zhou, and C. C. Seah, "Characterisation of underground blast-induced ground motions from large-scale field tests," *Shock Waves*, vol. 13, no. 3, pp. 237–252, 2003.

[14] B. Jayasinghe, Z. Zhao, A. G. Teck Chee, H. Zhou, and Y. Gui, "Attenuation of rock blasting induced ground vibration in rock-soil interface," *Journal of Rock Mechanics and Geotechnical Engineering*, vol. 11, no. 4, pp. 770–778, 2019.

[15] Z. Zhang, C. Zhou, A. Remennikov, T. Wu, S. Lu, and Y. Xia, "Dynamic response and safety control of civil air defense tunnel under excavation blasting of subway tunnel," *Tunnelling and Underground Space Technology*, vol. 112, Article ID 103879, 2021.

[16] R. He, *Dynamic Response Characteristic of Buildings Subjected to Blasting Excavation in Under-crossing Tunnels*, China University of Geosciences, Wuhan, China, 2018.

[17] L. B. Jayasinghe, H. Y. Zhou, A. T. C. Goh, Z. Y. Zhao, and Y. L. Gui, "Pile response subjected to rock blasting induced ground vibration near soil-rock interface," *Computers and Geotechnics*, vol. 82, pp. 1–15, 2017.

[18] N. Jiang, G. Lyu, T. Wu, C. Zhou, H. Li, and F. Yang, "Vibration effect and ocean environmental impact of blasting excavation in a subsea tunnel," *Tunnelling and Underground Space Technology*, vol. 131, Article ID 104855, 2023.

[19] R. Nateghi, "Prediction of ground vibration level induced by blasting at different rock units," *International Journal of Rock Mechanics and Mining Sciences*, vol. 48, no. 6, pp. 899–908, 2011.

[20] W. Lu, Y. Luo, M. Chen, and D. Shu, "An introduction to Chinese safety regulations for blasting vibration," *Environmental Earth Sciences*, vol. 67, no. 7, pp. 1951–1959, 2012.

[21] Y. Zeng, H. Li, X. Xia, B. Liu, H. Zuo, and J. Jiang, "Blast-induced rock damage control in Fangchenggang nuclear power station, China," *Journal of Rock Mechanics and Geotechnical Engineering*, vol. 10, no. 5, pp. 914–923, 2018.

[22] M. I. Matidza, Z. Jianhua, H. Gang, and A. D. Mwangi, "Assessment of blast-induced ground vibration at jinduicheng molybdenum open pit mine," *Natural Resources Research*, vol. 29, no. 2, pp. 831–841, 2020.

[23] M. Khandelwal and M. Saadat, "A dimensional analysis approach to study blast-induced ground vibration," *Rock Mechanics and Rock Engineering*, vol. 48, no. 2, pp. 727–735, 2015.

[24] N. Jiang, C. Zhou, S. Lu, and Z. Zhang, "Propagation and prediction of blasting vibration on slope in an open pit during underground mining," *Tunnelling and Underground Space Technology*, vol. 70, pp. 409–421, 2017.

[25] N. Jiang, B. Zhu, X. He, C. Zhou, X. Luo, and T. Wu, "Safety assessment of buried pressurized gas pipelines subject to blasting vibrations induced by metro foundation pit excavation," *Tunnelling and Underground Space Technology*, vol. 102, Article ID 103448, 2020.

[26] H. L. Langhaar, *Dimensional Analysis and Theory of Models*, Wiley, New York, NY, USA, 1951.